

Achievable Information Rates Estimation for 100-nm Raman-Amplified Optical Transmission System

Nikita A. Shevchenko, Tianhua Xu*, Daniel Semrau, Gabriel Saavedra, Gabriele Liga, Milen Paskov, Lidia Galdino, Alex Alvarado, Robert I. Killey, Polina Bayvel

Optical Networks Group, University College London (UCL), WC1E 7JE, London, United Kingdom, [*tianhua.xu@ucl.ac.uk](mailto:tianhua.xu@ucl.ac.uk)

Abstract *The achievable information rates of optical communication systems using ultra-wide bandwidth 100-nm distributed Raman amplification have been investigated for each individual sub-channels, based on the first-order perturbative analysis of nonlinear distortions.*

Introduction

To date, optical fibre communications have achieved unprecedented growth and success over the past three decades and now stand alone as the enabling technology that underpins the global information infrastructure. The data rates of optical communication systems have been raised from 100-Mbit/s per fibre in the 1970s to 10-Tbit/s in current commercial systems, an astonishing 100,000-fold increase. The key technologies that fueled this surge in capacity were wavelength division multiplexing (WDM), improved fibre design and fabrication, optical amplification and coherent detection. The use of Erbium-doped and Raman fibre amplifiers negated the need for electronic regenerators and enabled dense WDM transmission, although the success and performance of these amplifier technologies is seen as limiting the usable fibre bandwidth to approximately 10-15 THz, ultimately limiting the maximum throughput of optical systems.

Within the usable optical bandwidth, the increase of the spectral efficiency in Nyquist-spaced WDM systems is determined by the densest constellation that can be used. Denser constellations, however, typically operate well only at high signal-to-noise ratios (SNRs), where high optical launch power is required¹. In such schemes, the achievable information rate (AIR) of optical fibre communication systems is essentially limited by nonlinear (NL) distortions due to the optical Kerr effect manifesting itself as self-phase modulation, cross-phase modulation and four-wave mixing (FWM).

The AIRs have been evaluated for the total bandwidth of approximately the optical C-band (~4.3-THz) under the key assumption of ideally distributed Raman amplification schemes, while the Raman pump power and the distribution of the optical field-gain along the amplifier span have not been taken into account².

In this paper, for the first time to our

knowledge, the AIR of optical communication system using ultra-wideband optical Raman amplification extended to ~100-nm (12.51-THz) optical bandwidth in a standard single mode fiber (SSMF) has been numerically estimated by using a large-bandwidth first-order perturbative analysis of NL distortions. These estimations have been carried out separately for each sub-channel in Nyquist-spaced WDM transmission system. The AIR of the Raman-amplified transmission system with 1251-Channel \times 10-GHz using linear electronic dispersion compensation (EDC) and full-field (FF) nonlinear compensation (NLC) has been analysed. A first-order perturbative analysis was implemented to numerically evaluate the NL distortions for each individual sub-channel in Nyquist-spaced WDM transmission system, by removing the assumption of the "whiteness" of the NL distortion spectra.

Raman amplified optical system

Tab. 1: System parameter values

Parameters	Values
Num. of Channels (N_{ch})	1251
Symbol Rate (R_s)	10-Gbaud
Channel spacing ($\Delta\nu$)	10-GHz
Roll-off factor	0%
Total Raman pump power (P_p)	5×680 mW
Span length (L_s)	80 km
Fiber loss (α)	0.20 dB/km
Fiber loss for Raman pump (α_p)	0.25 dB/km
Dispersion (D)	17.0 ps/nm/km
Dispersion slope (S)	0.067 ps/nm ² /km
NL coefficient (γ)	1.20 1/W/km

We examine the backward-pumped geometry of optical Raman amplification. In this model, the Raman power gain is independent of the laser wavelength, and the pump depletion effect is neglected. The AIRs are evaluated in the optical communication system with distributed Raman amplification over ~100-nm (12.51-THz). We consider the transmission consisting of 1251 sub-channels with a symbol rate of 10-Gbaud and a channel spacing of 10-GHz. The detailed

parameters of the optical communication system are indicated in Tab. 1.

Analysis of nonlinear distortions for Raman amplified system

In optical communications, the performance of the WDM transmission system can be described by an effective SNR including both amplified spontaneous emission (ASE) and nonlinear interference noise contributions. This SNR can be approximated as

$$\text{SNR} \approx \frac{P}{P_N + P_{S-S} + P_{S-N}} \quad (1)$$

where P denotes the average launched power per channel, P_N is the total ASE noise of the transmission system, P_{S-S} is the total noise due to the nonlinear signal-signal interactions, and P_{S-N} is the total noise due to NL signal-ASE noise interaction.

For multi-span Nyquist-spaced WDM transmission systems, the total power of the ASE noise due to optical counter-pumped fibre Raman amplification can be calculated as

$$P_N = N_s N_p K_T \mathcal{N} \cdot h\nu_0 \cdot R_S \quad (2)$$

where N_s is the total number of spans in the optical link, N_p is the number of polarisation states, $K_T \approx 1.13$ is the temperature dependent phonon occupancy factor¹, $h\nu_0$ is the average photon energy at the optical carrier frequency, R_S is the symbol rate of the signal, \mathcal{N} represents the spontaneous emission noise photon number³.

For dual polarization (DP) Raman-amplified Nyquist-spaced WDM transmission system, the signal-signal NL interference power is defined as⁴

$$P_{S-S} = N_s^{\epsilon+1} \cdot \eta P^3 \quad (3)$$

where ϵ is the coherent factor which is between 0 and 1 depending on the decorrelation of NL distortions between each amplifier span⁴. The NL distortion coefficient η [W^{-2}] can be effectively modelled as follows

$$\eta(k) = \frac{1}{\Delta\nu} \int_{\frac{(2k-1)\Delta\nu}{2}}^{\frac{(2k+1)\Delta\nu}{2}} S(\nu) H(\nu) d\nu \quad (4)$$

$$S(\nu) \approx \frac{16\gamma^2}{27R_S^2} \iint_{-\frac{B}{2}}^{\frac{B}{2}} \Pi\left(\frac{\nu_1 + \nu_2 - \nu}{B}\right) \rho(\nu_1, \nu_2, \nu) d\nu_1 d\nu_2 \quad (5)$$

where $B = N_{\text{ch}} \cdot \Delta\nu$ represents the total WDM transmission bandwidth, $\Delta\nu$ is the channel spacing, γ is the fibre NL coefficient, and $\Pi(x)$ denotes the rectangular function. Eq. (4) implies the filtering of the PSD $S(\nu)$ in the coherent receiver by a matched filter with a baseband transfer function $H(\nu)$. The WDM channel index is given by the following set

$k = \left\{ -\frac{(N_{\text{ch}}-1)}{2}, \dots, \frac{(N_{\text{ch}}-1)}{2} \right\}$, where N_{ch} is the total number of WDM channels. $\rho(\nu_1, \nu_2, \nu)$ is the appropriate FWM efficiency factor, taking into account the Raman amplification⁵.

Finally, the signal-ASE noise interference term is given by⁶

$$P_{S-N} \approx 3\xi \cdot \eta P_N P^2 \quad (6)$$

where the factor ξ depends on the number of spans and can be approximated as follows

$$\xi \approx \frac{N_s^{\epsilon+1}}{2} + \frac{N_s^{\epsilon+2}}{\epsilon+2}. \quad (7)$$

Results and discussions

Due to the large bandwidth of the investigated signal, the Raman effect amplifies lower frequencies at the cost of higher frequencies during propagation. In order to prevent a large asymmetric power profile over the individual sub-channels, gain flattening filters will be employed at each span in practical applications. However, here we neglect the power redistribution and cross-talk resulting from intrapulse Raman scattering.

The NL distortion coefficient has been numerically computed for the central channel of WDM transmission system and its edges considering the slope of chromatic dispersion.

Tab. 2: NL distortions coefficient (η)

Nonlinear distortion coefficient $1/(\text{mW})^2$			
Ch. Index, k	-625	0	625
w/ β_3	0.0149	0.0275	0.0149
w/o β_3	0.0125	0.0276	0.0187

It can be seen according to the results of numerical calculations in Tab. 2 that the dispersion slope does not have a considerable impact on the NL distortions, e.g., setting β_3 to zero gives almost the same results, especially for the center channel. However, taking the slope into consideration substantially reduces the rate of convergence in the numerical integrations. Thus, we can fairly assume the negligibility of the dispersion slope throughout the paper without any significant loss in accuracy.

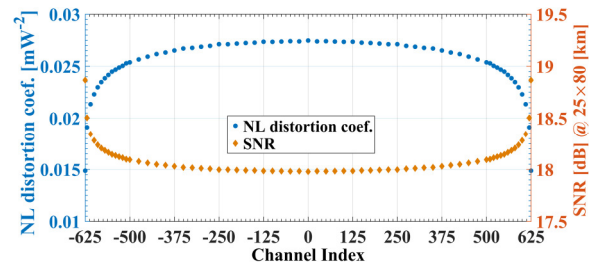


Fig. 1: Nonlinear distortion coefficient and SNR in Raman-amplified optical communication system

According to the above assumptions, the NL

distortion coefficients in the ~ 100 -nm Raman-amplified system have been numerically calculated for individual sub-channels. It can be seen in Fig. 1 that the nonlinear distortion coefficients in the outer channels are lower than those in the central sub-channels, physically due to less inter-channel NL distortion from neighboring channels. The differences become considerable when the channel index is outside the range -500 to $+500$. The SNR in each individual sub-channel has also been estimated based on the nonlinear distortion coefficients at 25×80 km using EDC, as shown in Fig. 1. In this case, the SNR difference between the central channel and the side channel is ~ 1 dB.

To obtain an indication of the AIR of the system, we compute soft-decision mutual information (MI) based on the Gaussian assumption on the channel. As detailed in⁷, this MI is an important figure of merit as it is a transmission rate that can be achieved by a receiver based on this Gaussian assumption.

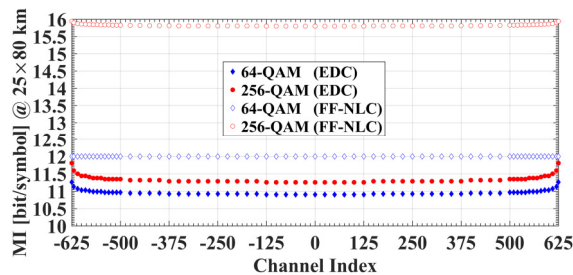


Fig. 2: Mutual information of individual sub-channels at 25×80 km transmission distance

The MI for each individual sub-channel was numerically calculated using Gauss-Hermite quadrature. We considered dual-polarization 64-QAM and 256-QAM, and both EDC and FF-NLC (the latter using ideal full-field digital back-propagation or optical phase conjugation). The obtained results for a transmission distance of 25×80 km are shown in Fig. 2. These results show that FF-NLC gives a significant improvement over EDC for 256-QAM. For 64-QAM the gains are smaller since the MIs for EDC are already close to their maximum value of 12 [bit/symbol].

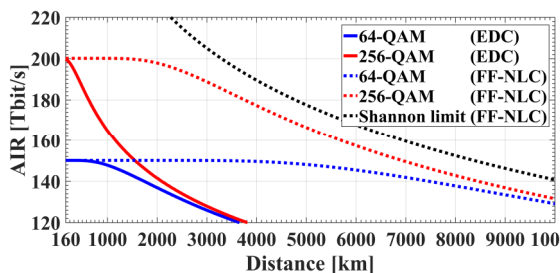


Fig. 3: Achievable information rates of 100-nm Raman amplified optical transmission system

Finally, to estimate the AIR over the entire bandwidth, the sub-channels were assumed to be independent, and thus, the total AIR was calculated as the sum of the MIs of each channel. Results were obtained for DP-64QAM and DP-256QAM under different transmission distances. These results are presented in Fig. 3 and show a significant improvement of FF-NLC over EDC for both modulation formats. The AIR for DP-256QAM exceeds 150-Tbit/s with linear EDC and 200-Tbit/s with FF-NLC for transmission distances of up to 1600 km.

Conclusions

The achievable information rates of optical fibre communication systems based on standard SMF and using ~ 100 -nm ultra-wideband optical Raman amplification has been numerically investigated using the first-order perturbative analysis of large-bandwidth NL distortions. The numerical estimations has been carried out for each individual sub-channel in Nyquist-spaced WDM transmission systems. It is estimated that ~ 100 -nm distributed Raman amplification gives the possibility of achieving AIRs of 150-Tbit/s using linear EDC, and 200-Tbit/s using FF-NLC over a transmission distance of 1600 km using DP-256QAM.

Acknowledgements

This work is supported by UK EPSRC project UNLOC (EP/J017582/1).

References

- [1] R. Essiambre, G. Kramer, P. J. Winzer, G. J. Foschini, and B. Goebel, "Capacity Limits of Optical Fiber Networks," *J. Lightwave Technol.*, Vol. **28**, no. 4, p. 662 (2010).
- [2] G. Bosco et al., "Analytical Results on Channel Capacity in Uncompensated Optical Links with Coherent Detection," *Opt. Express*, Vol. **19**, no. 26, p. B438 (2011).
- [3] S. R. Chinn, "Analysis of Counter-Pumped Small-Signal Fibre Raman Amplifiers," *Electron. Lett.*, Vol. **28**, no. 7, p. 607 (1997).
- [4] P. Poggiolini et al., "The GN-Model of Fiber Non-Linear Propagation and its Applications," *J. Lightwave Technol.*, Vol. **32**, no. 4, p. 694 (2014).
- [5] P. Poggiolini et al., "A Detailed Analytical Derivation of the GN model of Non-Linear Interference in Coherent Optical Transmission Systems," (2014). Available: <http://arxiv.org/abs/1209.0394>
- [6] D. Rafique, A. D. Ellis, "Impact of Signal-ASE Four-Wave Mixing on the Effectiveness of Digital Back-Propagation in 112 Gb/s PM-QPSK Systems," *Opt. Express*, Vol. **19**, no. 4, p. 3449 (2011).
- [7] T. Fehenberger, A. Alvarado, P. Bayvel, N. Hanik, "On Achievable Rates for Long-haul Fiber-Optic Communications," *Opt. Express*, Vol. **23**, no. 7, p. 9183 (2015).